

Submitted version, September 22, 1997
HUPD-9717, KUNS-1462

Evolution of Small Scale Cosmological Baryon Perturbations and Matter Transfer Functions

Kazuhiro Yamamoto¹

Department of Physics, Hiroshima University, Higashi-Hiroshima 739, Japan

and

Naoshi Sugiyama² & Humitaka Sato

Department of Physics, Kyoto University, Kyoto 606-01, Japan

ABSTRACT

The evolution of small scale cosmological perturbations is carefully re-examined. Through the interaction with photons via electrons, baryon perturbations show interesting behavior in some physical scales. Characteristic features of the evolution of baryon density fluctuations are discussed. In CDM models, it is found a power-law growing phase of the small-scale baryon density fluctuations, which is characterized by the *terminal velocity*, after the diffusion (Silk) damping and before the decoupling epoch. Then, a transfer function for total matter density fluctuations is studied by taking into account those physical processes. An analytic transfer function is presented, which is applicable for the entire range up to a solar mass scale in the high- z universe, and it is suitable also to the high baryon fraction models.

Subject headings: cosmology: theory – primordial density perturbations – cosmic structure formation

¹e-mail: yamamoto@astro.phys.sci.hiroshima-u.ac.jp

²e-mail: naoshi@tap.scphys.kyoto-u.ac.jp

1. Introduction

The structure formation in the high- z universe is one of the most important problem in the fields of cosmology and astrophysics. The structure formation of the Cold Dark Matter (CDM) dominated models is well motivated from the recent cosmological observations, e.g., from the microwave background anisotropies and the large scale structure of galaxies (White, Scott, & Silk 1994; Dodelson, Gates, & Turner 1996 ; Peacock & Dodds 1995), although it may require some modifications, i.e., inclusion of cosmological constant, and the tilted initial power spectrum with the gravity wave mode (White, Scott, Silk, & Davis 1995). We expect that the power spectrum of density fluctuations on scales $\gtrsim 1\text{Mpc}$ will be measured precisely in near future, e.g., from the 2DF survey, the Slon Digital Sky Survey (SDSS) project (see, e.g., Strauss 1996; Loveday 1996) and the future cosmic microwave background experiments with satellites ³ (see, e.g., Zaldarriaga, Spergel, & Seljak 1997; Jungman, Kamionkowski, Kosowsky, & Spergel 1996). These observations will severely constrain the cosmological parameters and the initial density power spectrum.

On the other hand, the inflation scenario provides a successful mechanism to explain the origin of cosmological density fluctuations. It predicts almost scale invariant and Gaussian fluctuations (Bardeen, Steinhardt, & Turner 1983). In this scenario, we expect that the initial density power spectrum extends up to very small scales. The evolution of density perturbations due to the fluctuations on very small scales is especially important for the early formation of the bound objects such as population III stars or primordial sub-galaxies for the hierarchical clustering scenario of the structure formation. By studying this evolution up to the non-linear regime with taking into account the heating and cooling processes, we would be able to learn the formation epoch and the formation process of the initial cosmic objects in the high- z universe (e.g., Ostriker & Gnedin 1996; Gnedin & Ostriker 1997; Haiman & Loeb 1997).

In this paper, we carefully re-examine the evolution of the small scale cosmological perturbations in the linear regime as an initial condition of the structure formation. In cosmological models with the high baryon fraction, the evolution of baryon density fluctuations affects that of the total matter fluctuations. This derives an alternation of the standard matter transfer function of the total matter density fluctuations. In particular, the power spectrum shows the damping on scales which are smaller than the Jeans scale at the decoupling epoch. This damping is caused by the acoustic oscillation of baryon perturbations. After describing these characteristic features of the evolution of baryon density fluctuations, we re-investigate the transfer function for the total matter density fluctuations.

In § 2, we give a brief review of the equations which describe the evolution of the cosmological perturbations. In § 3, we describe various physical scales which are relevant to the characteristic features of the evolution of baryon density fluctuations. The evolution of baryon density fluctuations

³ Planck home page <http://astro.estec.esa.nl/SA-general/Projects/Cobras/cobras.html>; MAP home page <http://map.gsfc.nasa.gov>.

before and after the decoupling are discussed in § 3 and § 4, respectively. The total matter transfer function is examined in § 5. In § 6, the accuracy of the transfer function is shown by calculating statistical quantities such as σ_8 . A physical implication of our results is also demonstrated by computing the formation rate of small bounded objects in the high- z universe based on the Press-Schechter theory. § 7 is devoted to summary and discussions. In Appendix A, we summarize the previous results on the CDM perturbations in small scales by Hu & Sugiyama (1996) (hereafter HS96). In Appendix B, we investigate the effect of the baryon thermal pressure on the transfer function on small scales after the decoupling.

Throughout this paper, we work in units where $c = \hbar = k_B = 1$. And we assume $T_0 = 2.726$ K as the cosmic microwave radiation temperature at present unless we explicitly include this valuable in equations.

2. Review of Formalism

Let us first summarize the equations which describe the evolution of the cosmological density perturbations on small scales. We write the perturbed metric in the Newtonian gauge,

$$ds^2 = \left(\frac{a}{a_0}\right)^2 \left(- (1 + 2\Psi)d\eta^2 + (1 + 2\Phi)d\mathbf{x}^2\right), \quad (1)$$

where Ψ is the perturbed gravitational potential, Φ is the curvature perturbation, a is the scale factor and the suffix 0 indicates the present value. As we are interested in the small scale cosmological perturbations, we can assume the geometry of the universe to be flat. We take into account the effect from the curvature term and the cosmological constant of the universe only near the present epoch through the change of the expansion rate. Then, in the high redshift universe, the Friedmann equation is written as,

$$H^2 = \left(\frac{\dot{a} a_0}{a a}\right)^2 = \left(\frac{a_0}{a}\right)^4 \frac{a_{\text{eq}} + a}{a_{\text{eq}} + a_0} \Omega_0 H_0^2, \quad (2)$$

where the dot denotes η -differentiation, H_0 is the Hubble constant, and a_{eq} is the scale factor at the matter-radiation equal-time. The Friedmann equation can be integrated as $k_{\text{eq}}\eta/2\sqrt{2} = (\sqrt{1 + a/a_{\text{eq}}} - 1)$, where we define $k_{\text{eq}}^2 = 2\Omega_0 H_0^2 (a_0/a_{\text{eq}})$, and

$$k_{\text{eq}} = 0.0948 \times \sqrt{1 - f_\nu} \Omega_0 h^2 \text{Mpc}^{-1}, \quad (3)$$

$$\frac{a_0}{a_{\text{eq}}} = 4.04 \times 10^4 (1 - f_\nu) \Omega_0 h^2, \quad (4)$$

with f_ν being the neutrino fraction in the energy density of radiations. For the massless standard neutrino model with three species, $f_\nu \simeq 0.405$.

The evolution of photon and neutrino radiation fields is described by the Boltzmann equation. The linearized evolution equation of the k -th Fourier mode of the photon temperature

perturbations is (see e.g., Kodama & Sasaki 1986; Hu & Sugiyama 1995, hereafter HS95),

$$\dot{\Theta} + ik\mu(\Theta + \Psi) = -\dot{\Phi} + \dot{\tau}\left(\Theta_0 - \Theta - \frac{1}{10}\Theta_2 P_2(\mu) - i\mu V_b\right), \quad (5)$$

where $\mu = \vec{\gamma} \cdot \mathbf{k}/|k|$, $\dot{\tau} = n_e \sigma_T a/a_0$, n_e is the free electron number density, σ_T is the Thomson cross section, $P_l(\mu)$ is the Legendre function, V_b is the velocity of baryon perturbations, Θ_l is defined by the multipole moment expansion of $\Theta(\eta, k, \vec{\gamma}) = \sum_{l=0}^{\infty} \Theta_l(\eta, k) (-i)^l P_l(\mu)$, and $\vec{\gamma}$ is the directional vector of the photon momentum. We can solve the equation using the multipole expansion method. The perturbations for the neutrino radiation fields obey to a similar equation. Effects of neutrino perturbations, however, are not so important for the structure formation on small scales. It should be taken into account only around the epoch of the horizon crossing (HS96).

In the fluid approximation, the evolution of CDM density fluctuations is described as

$$\dot{\delta}_c = -kV_c - 3\dot{\Phi}, \quad (6)$$

$$\dot{V}_c = -\frac{\dot{a}}{a}V_c + k\Psi, \quad (7)$$

where δ_c and V_c are the k -th Fourier mode of the perturbations of the CDM density contrast and the velocity, respectively.

In our gauge, the perturbed Einstein equation gives the extended Poisson equations,

$$k^2\Phi = 4\pi G\left(\frac{a}{a_0}\right)^2 \rho_T\left(\delta_T + 3\frac{\dot{a}}{a}(1 + w_T)k^{-1}V_T\right), \quad (8)$$

and

$$k^2(\Phi + \Psi) = -8\pi G\left(\frac{a}{a_0}\right)^2 p_T\Pi_T, \quad (9)$$

where $\rho_T(1 + w_T)V_T = \sum_x(\rho_x + p_x)V_x$, $w_T = P_T/\rho_T$, $\rho_T\delta_T = \sum_x\rho_x\delta_x$, the stress anisotropy is $\Pi_T = 12(\Theta_2 + N_2)/5$, Θ_2 and N_2 are the quadrupole anisotropies of the photon and the neutrino temperature perturbations.

We next consider the baryon-electron system. Electron(e), neutral and ionized hydrogen(H) and helium(He) are the particle species of the baryon-electron system. The number densities for each species are written as

$$n_e = x_e\left(1 - \frac{y_p}{2}\right)n_b, \quad n_H = (1 - y_p)n_b, \quad n_{He} = \frac{y_p}{4}n_b, \quad (10)$$

where y_p is the primordial helium mass fraction, n_H and n_{He} are the number densities of hydrogen and helium, respectively, $n_b = n_H + 4n_{He}$ is the total baryon number density, and $x_e = n_e/(n_H + n_{He})$ is the electron ionization fraction. We take a single fluid approximation for this baryon and electron system. Then the evolution equations of perturbations of the baryon-electron fluid can be written as

$$\dot{\delta}_b = -kV_b - 3\dot{\Phi}, \quad (11)$$

$$\dot{V}_b = -\frac{\dot{a}}{a}V_b + kc_s^2\delta_b + k\Psi + \dot{\tau}(\Theta_1 - V_b)/R, \quad (12)$$

where c_s is the sound velocity of the baryon-electron fluid, and $R \equiv 3\rho_b/4\rho_\gamma = 3\Omega_b/4\Omega_0(1 - f_\nu)^{-1}(a/a_{\text{eq}})$.

In the previous paper (Yamamoto, Sugiyama, & Sato 1997, hereafter YSS), we gave useful formulation for the small scale baryon perturbations. In particular we investigated how the Compton interaction between the electrons and the background photons determines the sound velocity of the baryon perturbations after the recombination. According to the previous result, the effective sound velocity of the baryon-electron fluid after the recombination can be determined by solving the dispersion relation,

$$-i\eta_E\omega(\omega^2 - c_f^2k^2) + \omega^2 - c_e^2k^2 = 0. \quad (13)$$

Here the real part of ω/k can be regarded as the effective sound velocity, i.e., $c_s = \text{Re}[\omega/k]$, η_E is the energy transfer time of the Compton interaction,

$$\eta_E^{-1} = \frac{8}{3} \frac{a}{a_0} \frac{x_e(1 - y_p/2)\sigma_T\rho_\gamma}{m_e(1 + x_e - (x_e + 3/2)y_p/2)}, \quad (14)$$

$c_f^2 = 5P_0/3\rho_b$, $c_e^2 = P_0/\rho_b$, P_0 and ρ_b are the pressure and the energy density of the baryon-electron fluid, respectively. Note that c_f is the sound speed for an adiabatic process and c_e for an isothermal process. The effective adiabatic index γ can be defined as $\gamma = c_s^2/c_e^2$. As is clear from equation (13), the effective sound velocity c_s (adiabatic index γ) is ruled by the ratio of the Compton energy transfer time scale η_E to the sound oscillation time scale. Namely, if $\eta_E\omega \ll 1$, then $\omega \simeq c_e k$ and $\gamma \simeq 1$. On the other hand, if $\eta_E\omega \gg 1$, $\omega \simeq c_f k$ and $\gamma \simeq 5/3$. Therefore the sound velocity depends on the wavelength of the perturbations, and γ is changed from 1 to 5/3 as the universe expands.

3. Evolution of the baryon perturbations before the decoupling

In this section, we describe the evolution of the cosmological baryon perturbations on small scales before the decoupling. The decoupling epoch (or the drag epoch) η_d of baryon perturbations is defined by $\tau_d(\eta_d, \eta_0) = 1$, where

$$\tau_d(\eta_1, \eta_2) \equiv \int_{\eta_2}^{\eta_1} d\eta \dot{\tau}(\eta)/R(\eta). \quad (15)$$

One can find the analytic fitting formula of this epoch in HS96. Note that this epoch is not necessarily equal to the last scattering epoch of photons which is defined by $\tau(\eta_{\text{rec}}, \eta_0) = 1$.

From the Compton interaction between electrons and photons, there are interesting varieties of physical scales for the baryon-electron fluid. In the previous paper (YSS), we summarized the details of the physical scales which are relevant to the evolution of baryon fluctuations. In this paper we focus on the small scale density perturbations, and describe the evolution using the physical scales. We define k^{phys} ($\lambda^{\text{phys}} \equiv 2\pi/k^{\text{phys}}$) as a physical wave number (wavelength), and k (λ) as a comoving wave number (wavelength). They are related as $k = (a/a_0)k^{\text{phys}}$ ($\lambda = (a_0/a)\lambda^{\text{phys}}$).

3.1. Horizon crossing and Jeans oscillation

The first characteristic scale is the horizon crossing scale in the evolution of perturbations. We define the horizon crossing scale by $1/k_{\text{H}} = \eta$, and the corresponding baryon mass scale by $M_{\text{H}} = 4\pi\rho_b(\pi/k_{\text{H}}^{\text{phys}})^3/3$. Then we have $M_{\text{H}} = 7.9 \times 10^{30}(1+z)^{-3}(1-f_\nu)^{3/2}\Omega_b h^2 M_\odot$, in the radiation dominated stage. According to this definition, the horizon crossing occurs at the redshift

$$1 + z_{\text{H}} = 2.0 \times 10^{10}(1 - f_\nu)^{1/2}(\Omega_b h^2)^{1/3}(M/M_\odot)^{-1/3}, \quad (16)$$

for perturbations with the baryon mass scale M . Since we have assumed that the perturbations cross the horizon in the radiation dominated stage, this expression is applicable for $M \ll 1.2 \times 10^{17}(1 - f_\nu)^{-3/2}\Omega_b h^2(\Omega_0 h^2)^{-3} M_\odot$.

The next important scale is the Jeans scale. Since the coupling between baryons and photons is tight due to the Compton interaction sufficiently before recombination, the photon-pressure prevents perturbations from collapsing. Therefore the baryon-photon perturbations oscillate as an acoustic wave inside the Jeans scale. We define the Jeans wavelength (wave number) before recombination by $\lambda_{\text{J}}^{\text{phys}} = 2\pi/k_{\text{J}}^{\text{phys}} \equiv (\pi c_s^2/G(\rho_m + \rho_\gamma))^{1/2}$, where $\rho_m = \rho_b + \rho_c$ and ρ_c is the energy density of CDM. Defining the Jeans mass as $M_{\text{J}} = 4\pi\rho_b(\lambda_{\text{J}}^{\text{phys}}/2)^3/3 = 4\pi\rho_b(\pi/k_{\text{J}}^{\text{phys}})^3/3$, we get

$$M_{\text{J}} = 8.6 \times 10^{29}(1+z)^{-3}\Omega_b h^2 M_\odot, \quad (17)$$

in the radiation dominated stage. Then the Jeans crossing occurs at redshift,

$$1 + z_{\text{J}} = 9.4 \times 10^9(\Omega_b h^2)^{1/3}(M/M_\odot)^{-1/3}, \quad (18)$$

for the perturbations with the baryon mass M , which is right after the horizon crossing epoch. Since we have assumed perturbations cross the Jeans scale in the radiation dominated stage, this expression is applicable for $M \ll 10^{16}\Omega_b h^2(\Omega_0 h^2)^{-3} M_\odot$. When the coupling between baryons and photons is tight, the baryon-photon system behaves as a single fluid. The oscillation is expressed in the analytic form,

$$\delta_b = \frac{9}{2}\left(1 + \frac{2}{5}f_\nu\right)^{-1} \Phi(0, k)(1 + R)^{-1/4} \cos(kr_s), \quad (19)$$

for adiabatic perturbations (HS95;HS96), where $r_s = \int_0^\eta d\eta'/\sqrt{3(1+R)}$, and $\Phi(0, k)$ is the initial curvature perturbation.

Figure 1 shows the numerical evolution of baryon and CDM density fluctuations with various baryon mass scales, $10^{12}M_\odot$, 10^9M_\odot , 10^6M_\odot , and 10^3M_\odot . It is apparent from the figure that baryon density fluctuations start oscillating after the Jeans crossing. It is also well known that CDM density fluctuations grow logarithmically after the horizon crossing in the radiation dominant regime (see e.g., HS96). Moreover, this figure shows some prominent features of the evolution of baryon density fluctuations, i.e., damping, re-growth and catching up with CDM density fluctuations. These are discussed in the following subsections and §4.

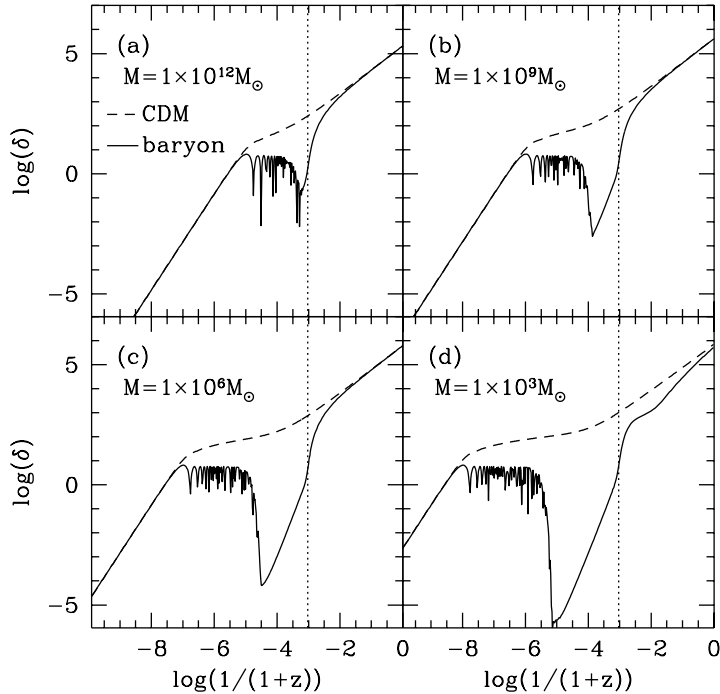


Fig. 1.— Typical numerical evolution of baryon and the CDM density fluctuations, δ_b (solid lines) and δ_c (dashed lines), with baryon mass scales $10^{12}M_\odot$, 10^9M_\odot , 10^6M_\odot , and 10^3M_\odot , respectively. These mass scales correspond to the wave numbers $k = 9.65 \times 10^{-1}, \times 10^0, \times 10^1$, and $\times 10^2 \text{Mpc}^{-1}$, respectively. Note that here we employ the gauge to set the total matter center-of-mass frame, instead of the Newtonian gauge for the convenience of numerical calculations. The behavior of fluctuations inside the horizon does not depend on the gauge choice. We chose the cosmological parameters, $h = 0.5$, $\Omega_0 = 1.0$, and $\Omega_b = 0.1$. The dotted line shows the decoupling time of baryons and photons. We see the power-law growing phase of baryon density fluctuations after the diffusion damping before the decoupling. After the decoupling the baryon fluctuations catch up with CDM fluctuations through the gravitational free fall, unless the perturbations are smaller than the Jeans scale (see panel (d)).

3.2. Diffusion damping and the breaking scale of the tight coupling approximation

It is well known that the photon diffusion process erases the baryon-photon perturbations on small scales (Silk 1968; Sato 1971; Weinberg 1971). This damping length is the random walk distance of a photon scattered by electrons through the Compton interaction. The mean free path of a photon is $1/\dot{\tau}$. The integrated distance that the photon proceeds is the horizon scale η in terms of the comoving length. Hence this damping scale is roughly expressed as $l \simeq \sqrt{\eta/\dot{\tau}}$. In a more detailed treatment, we define the damping scale by k_D , where $k_D^{-2} = \int_0^\eta d\eta' (R^2 + 8(1+R)/9)/(6\dot{\tau}(1+R)^2)$ (see e.g., HS95). It is known that the exponential damping factor, $\exp[-k^2/k_D^2]$ is multiplied to the right hand side of equation (19) to describe this damping feature. Correspondingly, the baryon mass scale of the diffusion damping is defined by $M_D = 4\pi\rho_b(\pi/k_D^{\text{phys}})^3/3$, which reduces to

$$M_D = 1.4 \times 10^{27} (1+z)^{-9/2} (1-y_p/2)^{-3/2} (1-f_\nu)^{3/4} (\Omega_b h^2)^{-1/2} M_\odot. \quad (20)$$

For the perturbations with the baryon mass scale M , this damping occurs at redshift

$$1 + z_D = 1.1 \times 10^6 (1 - f_\nu)^{1/6} (1 - y_p)^{-1/3} (\Omega_b h^2)^{-1/9} (M/M_\odot)^{-2/9} . \quad (21)$$

Here we have assumed this regime to be sufficiently before recombination.

Now let us examine the validity of the tight coupling approximation for the baryon-photon system. When the photon mean free path crosses over the wavelength of the perturbations, the tight coupling approximation for the baryon-photon system cannot be applicable anymore. We define this breaking scale of the tight coupling approximation by $1/k_{\text{BR}}^{\text{phys}} = \lambda_{\text{BR}}^{\text{phys}}/2\pi = 1/n_e \sigma_T$. The corresponding baryon mass scale is defined by $M_{\text{BR}} = 4\pi\rho_b(\pi/k_{\text{BR}}^{\text{phys}})^3/3$, which reduces to

$$M_{\text{BR}} = 2.9 \times 10^{27} (1 + z)^{-6} (1 - y_p/2)^{-2} (\Omega_b h^2)^{-2} M_\odot , \quad (22)$$

where we have used $x_e = 1$ assuming the regime sufficiently before recombination. Accordingly, the tight coupling approximation breaks down at redshift

$$1 + z_{\text{BR}} = 3.8 \times 10^4 (1 - y_p)^{-1/2} (\Omega_b h^2)^{-1/3} (M/M_\odot)^{-1/6} , \quad (23)$$

for the perturbations with the baryon mass scale M . Extrapolating equation (22) until the decoupling epoch ($z \simeq 1000$), we obtain $M_{\text{BR}} = 2.9 \times 10^9 ((1 + z)/1000)^{-6} (1 - y_p/2)^{-2} (\Omega_b h^2)^{-2} M_\odot$.

In Figure 2 we show the physical baryon mass scales described in the above. As can be read from this figure, the tight coupling approximation breaks down after the diffusion damping but sufficiently before recombination on small scales. Next we study the effect of this tight coupling breaking on the evolution of density fluctuations.

3.3. Evolution of baryon fluctuations by the terminal velocity

In Figure 1, which is obtained by numerical computations, we find the power-law growing phase of baryon fluctuations after the diffusion damping but sufficiently before the decoupling on small scales. This evolution of baryon fluctuations is characterized as follows. Equation (12) has the formal solution

$$aV_b(\eta) = \int_0^\eta d\eta' a \left(\frac{\dot{\tau}}{R} \Theta_1 + kc_b^2 \delta_b + k\Psi \right) e^{-\tau_d(\eta', \eta)} , \quad (24)$$

where $\tau_d(\eta', \eta) = \int_{\eta'}^\eta d\tilde{\eta} \dot{\tau}(\tilde{\eta})/R(\tilde{\eta})$. Since the diffusion damping erases baryon-photon perturbations, the dominant term in the integrant of the right hand side of equation (24) is the gravitational force term. Therefore we can approximate $aV_b(\eta) \simeq \int_0^\eta d\eta' ak\Psi e^{-\tau_d(\eta', \eta)}$. Before the decoupling, the optical depth $\tau_d(\eta', \eta)$ is a quite large number, and the time variation of $e^{-\tau_d(\eta', \eta)}$ is extremely rapid. Thus we approximate as $e^{-\tau_d(\eta', \eta)} \simeq e^{-(\eta - \eta')\dot{\tau}(\eta)/R(\eta)}$, and neglect the time dependence of Ψ , which derives

$$V_b(\eta) \simeq k\Psi \frac{R}{\dot{\tau}} . \quad (25)$$

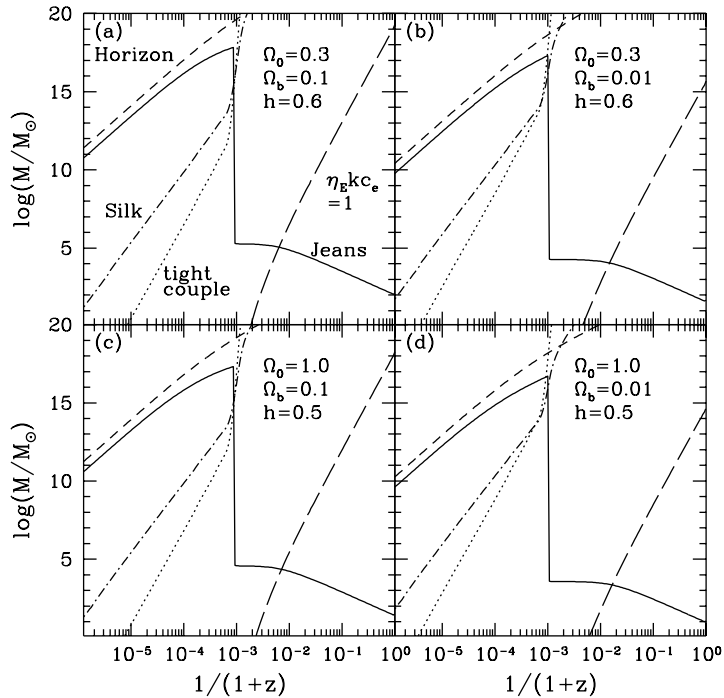


Fig. 2.— Physical mass scales of baryon perturbations for several different cosmological parameters. In this figure, ‘Horizon’ (short dashed lines), ‘Jeans’ (solid lines), ‘Silk’ (dot-dashed lines) and ‘tight couple’ (dotted lines) represent the horizon scale, the Jeans scale, the diffusion (Silk) damping scale, and the breaking scale of the tight coupling approximation of baryon and photon fluids. Long dashed lines are the lines on which the Compton energy time is equal to the sound oscillation time scale, i.e., $\eta_E k c_e = 1$.

We can verify that this relation holds quite well during the power-law growing phase as is shown in Figure 3. We will discuss this figure in detail later in this subsection. The above relation is also obtained by equating the gravitational force due to the potential of CDM fluctuations, $k\Psi$, and the friction force due to the interaction with background photons, $\dot{\tau}V_b/R$, in the right hand side of equation (12). Thus this relation implies the balance of these two forces for baryon perturbations. Therefore this baryon velocity can be referred as the *terminal velocity*. This is the result of the breaking of the tight coupling approximation. After the epoch $\tau_d \lesssim 1$, the baryon velocity is induced by the gravitational free fall, i.e., $V_b(\eta) = a^{-1} \left(\int_{\eta_d}^{\eta} d\eta' a k \Psi + a_d V_b(\eta_d) \right)$. Therefore the power-law growth by the terminal velocity lasts by the end of the baryon drag epoch.

Let us discuss this growing feature of the evolution by the terminal velocity more quantitatively. In the matter dominant stage, the time variation of the curvature perturbation can be neglected. In this case, baryon density fluctuations are given by $\delta_b(\eta) \simeq -k^2 \Psi(\eta) \int^{\eta} d\eta' R/\dot{\tau}$, from equations

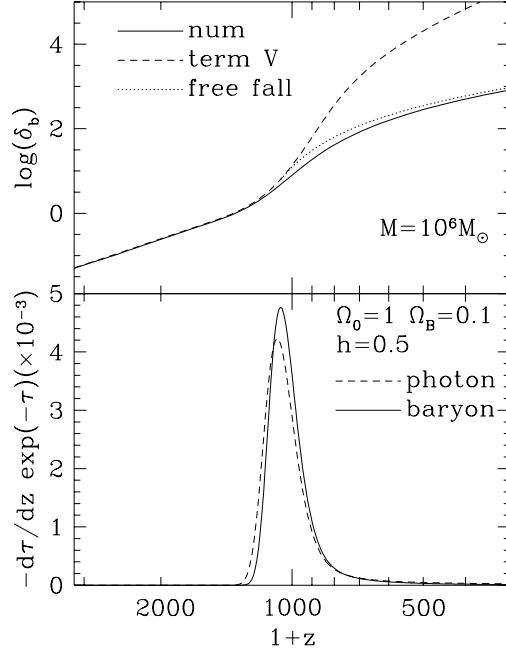


Fig. 3.— Evolution of baryon density fluctuations and the visibility function around the decoupling epoch. The upper panel shows the evolution of baryon density fluctuations with the baryon mass scale $10^6 M_\odot$ which corresponds to $k = 96.5 \text{Mpc}^{-1}$ (see panel (c) of Figure 1). The cosmological parameters are same as Figure 1. In this panel, ‘num’ (a solid line), ‘term V’ (a dashed line), and ‘free fall’ (a dotted line) represent fully numerical computation, the semi-analytic computation with setting $V_b = k\Psi R/\dot{\tau}$, i.e., fluctuations induced by the terminal velocity, and the semi-analytic computation with setting V_b to evolve via gravitational free fall after the decoupling. The lower panel shows the corresponding visibility functions. Note that the last scattering epoch, which is the location of the peak of the visibility function, of photons (a dashed line) and baryons (a solid line) are not completely the same. We refer the latter as a decoupling epoch in this paper. It is shown in this figure that the semi-analytic calculation starts to deviate from the numerical calculations at which the decoupling process takes place (see the thickness of the visibility function).

(11) and (25). Assuming $x_e = 1$, we have $R/\dot{\tau} = 3.0 \times 10^4 \Omega_b h^2 / (n_e \sigma_T)$. Then we can derive

$$\delta_b(\eta) \simeq -0.32(1 - f_\nu)(1 - y_p/2)^{-1}(\Omega_0 h^2)^{3/2} \left(\frac{1000}{1+z}\right)^{7/2} \left(\frac{k}{k_{\text{eq}}}\right)^2 \Psi(\eta). \quad (26)$$

It should be noticed that this relation is applicable between the breaking epoch of the tight coupling and the decoupling epoch. The ratio of baryon density fluctuations to CDM ones is written as

$$\frac{\delta_b(\eta)}{\delta_c(\eta)} \simeq 0.7 \times 10^{-2} (\Omega_0 - \Omega_b) \Omega_0^{-1/2} h \left(\frac{1000}{1+z}\right)^{5/2}, \quad (27)$$

where we took $y_p = 0.23$, since CDM density fluctuations can be written as

$$\delta_c(\eta) \simeq -5.4 \times 10 (1 - f_\nu) \frac{\Omega_0^2 h^2}{\Omega_0 - \Omega_b} \left(\frac{1000}{1+z}\right) \left(\frac{k}{k_{\text{eq}}}\right)^2 \Psi(\eta), \quad (28)$$

which is obtained from the relation $k^2\Psi \simeq -4\pi G(a/a_0)^2\rho_c\delta_c$. From equation (27), it is found that the ratio of baryon density fluctuations to CDM ones does not depend on the wave number k before the decoupling epoch.

Since the above estimation is rather crude, we investigate the behavior around the decoupling epoch in more detail. Equation (26) is a good approximation for δ_b before the decoupling epoch. However, we cannot employ equation (26) during the decoupling epoch, because the decoupling process occurs in the finite time duration and our assumption of the fully ionization breaks down. Figure 3 shows the evolution of baryon fluctuations and the corresponding baryon and photon visibility functions (HS96). In the upper panel, the solid line shows the evolution obtained from the fully numerical computation. The dashed line shows the evolution of the baryon fluctuations with setting the baryon velocity to be the terminal velocity, i.e., $V_b = k\Psi R/\dot{\tau}$. The dotted line shows the evolution with setting that $V_b = k\Psi R/\dot{\tau}$ until the decoupling z_d defined in HS96, and setting V_b to follow the free fall solution, i.e., $\dot{V}_b = -V_b(\dot{a}/a) + k\Psi$ after the decoupling. From this figure, it is apparent that our simple picture such that the small scale baryon fluctuations grow via the terminal velocity until the decoupling epoch, and they grows via gravitational free fall after that, works remarkably well before the decoupling epoch and works fairly well after the decoupling epoch. However, there appears a small discrepancy during the decoupling epoch, i.e., within the thickness of the visibility function (see the lower panel). The evolution of baryon fluctuations accelerates as the decoupling process begins. However the actual acceleration is not as fast as the one which is given by the terminal velocity (see the dashed line). This is because the friction between baryons and photons is getting smaller as the universe becomes transparent. If the friction force and gravitational force were still balanced, unrealistically large velocity would be required. Therefore we overestimate the velocity if we employ the terminal velocity during and after the decoupling epoch. This is why the dashed line exceeds the numerical one (the solid line) at the decoupling time z_d which is the peak location of the baryon visibility function. Moreover, we have entirely ignored the friction (or drag) term after z_d in our semi-analytic calculation. Therefore we expect the dotted line is larger than the numerical one as is shown in Figure 3. After the decoupling epoch, however, the dotted line gradually overlaps with the numerical one. We note that this overlapping occurs earlier if we include the drag effect by photons after z_d in our free fall calculation.

On the other hand, if we employ equation (26) by the decoupling time z_d , we underestimate the amplitude of baryon fluctuations. Therefore the actual ratio between baryon and CDM density fluctuations is lower than the value of equation (27). Nevertheless, baryon density fluctuations have the amplitude of $O(10^{-3}) \sim O(10^{-2})$ relative to CDM fluctuations on small scales at the decoupling epoch. As we have already mentioned that this ratio does not depend on the wavenumber k . These features can be seen in Figure 1. Since this ratio is fairly small, the assumption by HS96, that is to set the baryon density fluctuations to be zero after the damping epoch, is verified. Therefore we can employ their formulas of the evolution of CDM density fluctuations although some modifications are required on very small scales where the wave length of baryon perturbations is smaller than the

Jeans scale after the decoupling epoch.

4. Evolution of baryon density fluctuations after the decoupling

In this section we investigate the evolution of density fluctuations after the decoupling epoch. Baryon density fluctuations are catching up with CDM density fluctuations after the decoupling, as is shown in Figure 1. The important physical scale which is relevant to this feature is the Jeans scale. We define the Jeans wavelength (wave number) after the decoupling by $\lambda_J^{\text{phys}} = 2\pi/k_J^{\text{phys}} = \sqrt{\pi c_s^2/G\rho_m}$. Then we have $k_J = 1.3 \times 10^3(1+z)^{1/2}(\gamma\xi T_b)^{-1/2}(\Omega_0 h^2)^{1/2} \text{ Mpc}^{-1}$, where T_b is the baryon matter temperature in unit of Kelvin, and $\xi = 1 - 3y_p/4$. Correspondingly, the baryon mass scale is defined by $M_J = 4\pi\rho_b(\pi/k_J^{\text{phys}})^3/3$, which is written as

$$M_J = 1.5 \times 10^4(1+z)^{-3/2}(\gamma\xi T_b)^{3/2}(\Omega_0 h^2)^{-3/2}\Omega_b h^2 M_\odot . \quad (29)$$

Thus the epoch when the Jeans scale becomes smaller than the scale of fluctuations with M is

$$1 + z_J^{\text{out}} = 6.1 \times 10^2 \gamma\xi T_b (\Omega_0 h^2)^{-1} (\Omega_b h^2)^{2/3} (M/M_\odot)^{-2/3} . \quad (30)$$

As is shown in Figure 2, the Jeans scale after the decoupling has the plateau. In this stage, the energy transfer between background photons and the baryon fluid is effective through the residual electrons, and the baryon temperature follows the photon temperature. As the universe expands, however, the energy transfer time rises above the Hubble expansion time. After that epoch, the baryon matter temperature cools adiabatically and drops as $T_b \propto a^{-2}$, which derives the decrease of the Jeans scale. Thus the Hubble expansion time scale and the Compton energy transfer time scale is equal at the broken corner of the plateau of the Jeans scale. This epoch is estimated as $(1+z) \simeq 1000(\Omega_b h^2)^{2/5}$ (Peebles 1993). It is interesting that this redshift depends only on the parameter $\Omega_b h^2$. The line of $\eta_E k c_e = 1$, on which the Compton energy time is equal to the sound oscillation time scale, crosses at the broken corner of the plateau of the Jeans scale. Thus this cross point of two lines is the point when the sound oscillation time, the Hubble expansion time and the energy transfer time become all the same (YSS).

This constant value of the Jeans scale, which is the maximum Jeans scale at the decoupling epoch, gives a characteristic scale of baryon perturbations. From the definition, this Jeans scale is written as $k_{\text{JP}} = 9.0 \times 10^2(\Omega_0 h^2)^{1/2}\text{Mpc}^{-1}$. Correspondingly, the baryon mass is

$$M_{\text{JP}} = 5.0 \times 10^4(\Omega_0 h^2)^{-3/2}\Omega_b h^2 M_\odot . \quad (31)$$

Here we have set $y_p = 0.23$ and $f_\nu = 0.405$, which we use in the hereafter. According to the usual picture of the Jeans oscillation, baryon perturbations whose scale are smaller than this characteristic scale are kept from growing by the baryon thermal pressure. On the other hand, the density fluctuations larger than this characteristic scale can grow by the gravitational infall into CDM potential wells, and catch up to the CDM density fluctuations. The time scale of this infall process is described by the free fall time.

By using the fitting formula, $T_b = 4.5 \times 10^{-3} (1+z)^2 (\Omega_b h^2)^{-2/5}$ K, which represents the baryon matter temperature after the energy transfer between baryons and photons becomes ineffective (YSS), we find that the epoch when the perturbations with the wave number k ($> k_{\text{JP}}$) cross the Jeans scale is at redshift

$$1 + z_J^{\text{out}} = 2.9 \times 10^8 (k \text{ Mpc})^{-2} \Omega_0 h^2 (\Omega_b h^2)^{2/5}. \quad (32)$$

This epoch is rewritten in terms of the scale factor as

$$y_J^{\text{out}} \equiv a_J^{\text{out}}/a_{\text{eq}} = 8.2 \times 10^{-5} (k \text{ Mpc})^2 (\Omega_b h^2)^{-2/5}. \quad (33)$$

This is the second Jeans crossing time for the perturbations with $k > k_{\text{JP}}$. These perturbations once cross the Jeans scale at z_J of equation (18) before the decoupling epoch and starts to oscillate as acoustic waves. Then again they cross the Jeans scale at z_J^{out} and are catching up with the CDM density fluctuations due to gravitational infall.

5. Transfer Function

It will be convenient to recast the evolutionary effects in terms of a transfer function of density fluctuations. In the present paper, we consider the transfer function of matter density fluctuations which are defined by

$$\delta_m = \frac{\Omega_c}{\Omega_0} \delta_c + \frac{\Omega_b}{\Omega_0} \delta_b, \quad (34)$$

with $\Omega_c = \Omega_0 - \Omega_b$. The transfer function can be defined by

$$T_m(a, k) = \frac{\delta_m(a, k)}{\lim_{k \rightarrow 0} \delta_T(a, k)}, \quad (35)$$

where δ_T is the total transfer function with radiation contributions. In the matter dominate stage, $\delta_m \simeq \delta_T$. Using the large scale solution (HS95), we obtain

$$\lim_{k \rightarrow 0} \delta_m(a, k) = \left(1 + \frac{4}{15} f_\nu\right) \left(1 + \frac{2}{15} f_\nu\right)^{-1} \frac{6}{5} \left(\frac{k}{k_{\text{eq}}}\right)^2 \Phi(0, k) D_1(a), \quad (36)$$

where $D_1(a) = 2/3 + a/a_{\text{eq}}$. In general, the transfer function is a function of time. However, once the pressure term of baryon perturbations becomes negligible at some scale, $\delta_m \propto D_1(a)$ (Peebles 1980; see also equation (A8)). Then the transfer function (35) becomes independent of time at this scale. Therefore we can assume the time invariance of the transfer function after the decoupling epoch on scales larger than the maximum Jeans scale after the decoupling, i.e., $k < k_{\text{JP}}$ or after z_J^{out} on $k > k_{\text{JP}}$.

While the transfer function by Bardeen, et al. (1986, hereafter BBKS) is familiar, the effect of the baryon fraction is not taken into account. This transfer function is not applicable for models with non-negligible baryon fraction at $k \gtrsim 0.1 \Omega_b^{1/2} \Omega_0^{1/2} h^2 \text{Mpc}^{-1}$. The effects of the baryon

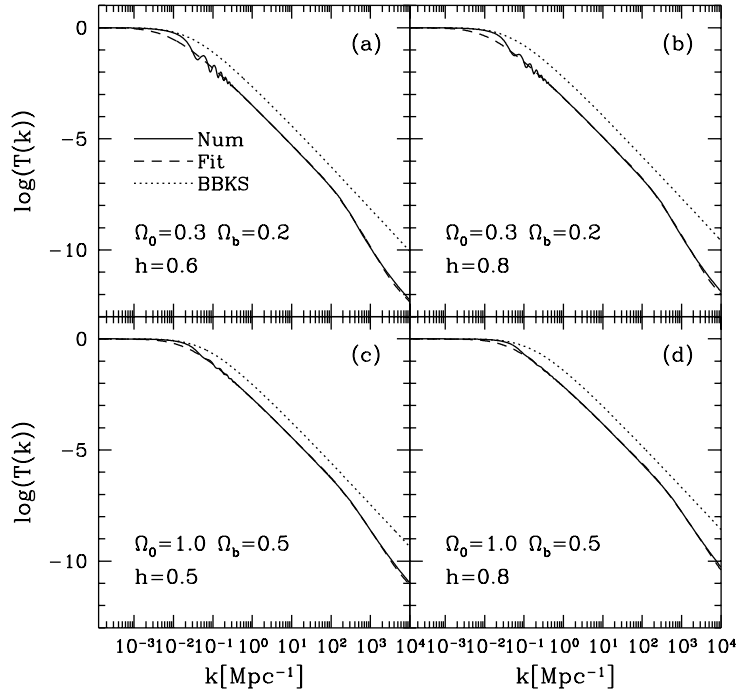


Fig. 4.— Transfer functions $T_m(k)$ at present. They are obtained by Numerical calculations (solid lines), analytic fitting (dashed lines) and BBKS fitting (dotted lines), respectively.

fraction on the large-scale power spectrum have been investigated by Holtzman (1989), Peacock & Dodds (1995), and Sugiyama (1995). The effects of the baryon fraction on the transfer function is incorporated by simply scaling of so-called Γ factor of the BBKS transfer function⁴. However, errors arise on scales smaller than the galaxy scale. In Figure 4, the fitting formula of the transfer function and the numerical computation described below are compared with the BBKS transfer function. Here the deviation is exaggerated by considering the cosmological models with high baryon density fraction. HS96 have investigated the CDM transfer functions on very small scales. Their result is summarized in the first part of Appendix B. In their paper, the effect of the baryon fraction is taken into account and they have given the transfer function in an analytic form. Though it is rather complicated equation, it has a high accuracy even for high baryon density models. However, there are following limitations in their transfer function. First, their transfer function is limited only on very small scales ($k \gtrsim 1\text{Mpc}$), and it is not applicable at the scales larger than the galaxy

⁴In a recent paper by Eisenstein & Hu (1997), they obtained better scaling, which includes k dependence, to fit intermediate scale ($\sim 100\text{Mpc}$). Moreover, they presented very detailed and precise, but complicated, fitting formula of the transfer function on large scales ($k \lesssim 1\text{Mpc}^{-1}$) with taking into account the acoustic oscillations of the photon-baryon fluid before the decoupling epoch. Although their paper appears after writing up this paper, we decide to mention their transfer function in the following sessions.

scale. Secondly, they do not take into account the Jeans oscillation of baryon fluctuations after the decoupling epoch. Therefore their transfer function cannot apply at the wave number larger than k_{JP} . Here we propose an analytic transfer function which is useful for the entire region of wavelength.

The transfer function which we propose is following:

$$T_{\text{m}}(a, k) = \frac{\ln(1 + 2.34\tilde{q}(1 + \kappa\tilde{q})/(1 + \tilde{q}))}{2.34\tilde{q}[1 + 3.89\tilde{q} + (16.1\tilde{q})^2 + (5.46\tilde{q})^3 + (6.71\tilde{q})^4]^{1/4}} f_{\text{m}}(a, k), \quad (37)$$

with

$$\tilde{q} = 0.951(\alpha\Omega_{\text{c}}/\Omega_0)^{-1/2} \frac{k\text{Mpc}}{\Omega_0 h^2} \Theta_{2.7}^2, \quad (38)$$

$$\kappa = 0.809(\alpha\Omega_{\text{c}}/\Omega_0)^{1/2} \beta, \quad (39)$$

where $\Theta_{2.7} = T_0/2.7\text{K}$, α and β are defined in equation (B2), and $f_{\text{m}}(a, k)$ in equation (B7) in Appendix B. Except for $f_{\text{m}}(a, k)$, the transfer function is obtained by incorporating the small scale transfer function in HS96 into the familiar formula of BBKS with scaling. The large scale behavior of the transfer function at $k \sim 0.1\text{Mpc}^{-1}$ is successfully expressed by BBKS transfer function with simple scaling (Sugiyama 1995). However, the small scale behavior is not satisfactory. It is required that the transfer function approaches to the form in HS96 in the small scale limit. The term in the logarithm in equation (37) plays a role to change from large scale formula to the small scale one.

Let us briefly comment on the correction factor $f_{\text{m}}(a, k)$, which is described in detail in Appendix B. As discussed in §4, the maximum Jeans scale after the decoupling epoch is expressed by k_{JP} . The baryon thermal pressure keeps baryon fluctuations from growing even after the decoupling epoch on the scales $k > k_{\text{JP}}$. When baryon fluctuations can not grow and remain the small amplitude, the growth rate of CDM density fluctuations is suppressed. In this stage, the growth rate of CDM fluctuations is roughly in proportion to $(1 + a/a_{\text{eq}})^{-\alpha_1}$ with $\alpha_1 = (1 - \sqrt{1 + 24(\Omega_0 - \Omega_{\text{b}})/\Omega_0})/4$. Eventually this effect decreases the transfer function on sales smaller than k_{JP} after the decoupling. In order to describe this effect, we introduce the window function $f_{\text{m}}(a, k)$.

In Figure 5, the fitting formula of the transfer function is compared with the numerical computation, normalized to the BBKS transfer function. Our fitting formula reproduces the numerical result quite well for the scale, $1\text{Mpc}^{-1} \lesssim k \lesssim 100\text{Mpc}^{-1}$, within a few percent for $0.5 \lesssim h \lesssim 0.8$ and $\Omega_{\text{b}}/\Omega_0 \lesssim 0.5$. For the smaller scales $k \gtrsim 100\text{Mpc}^{-1}$, where $f_{\text{m}}(a, k)$ becomes important, our fitting function works within $\sim 10\%$ accuracy at $z \lesssim 100$. For the larger scales $k \lesssim 0.1\text{Mpc}^{-1}$, the numerical transfer function shows the feature with bumps and wiggles due to the baryon-photon acoustic oscillation before the decoupling. The larger the baryon fraction is, the bigger this effect becomes. As we do not take this effect into account, the difference between the fitting formula and the numerical result becomes large. However, the fitting formula still designs to cross the center of these oscillations. Therefore we expect fairly good fit with the observational quantities, such as

σ_8 . The accuracy of the fitting formula is checked in the next section in more detail by computing statistical quantities.

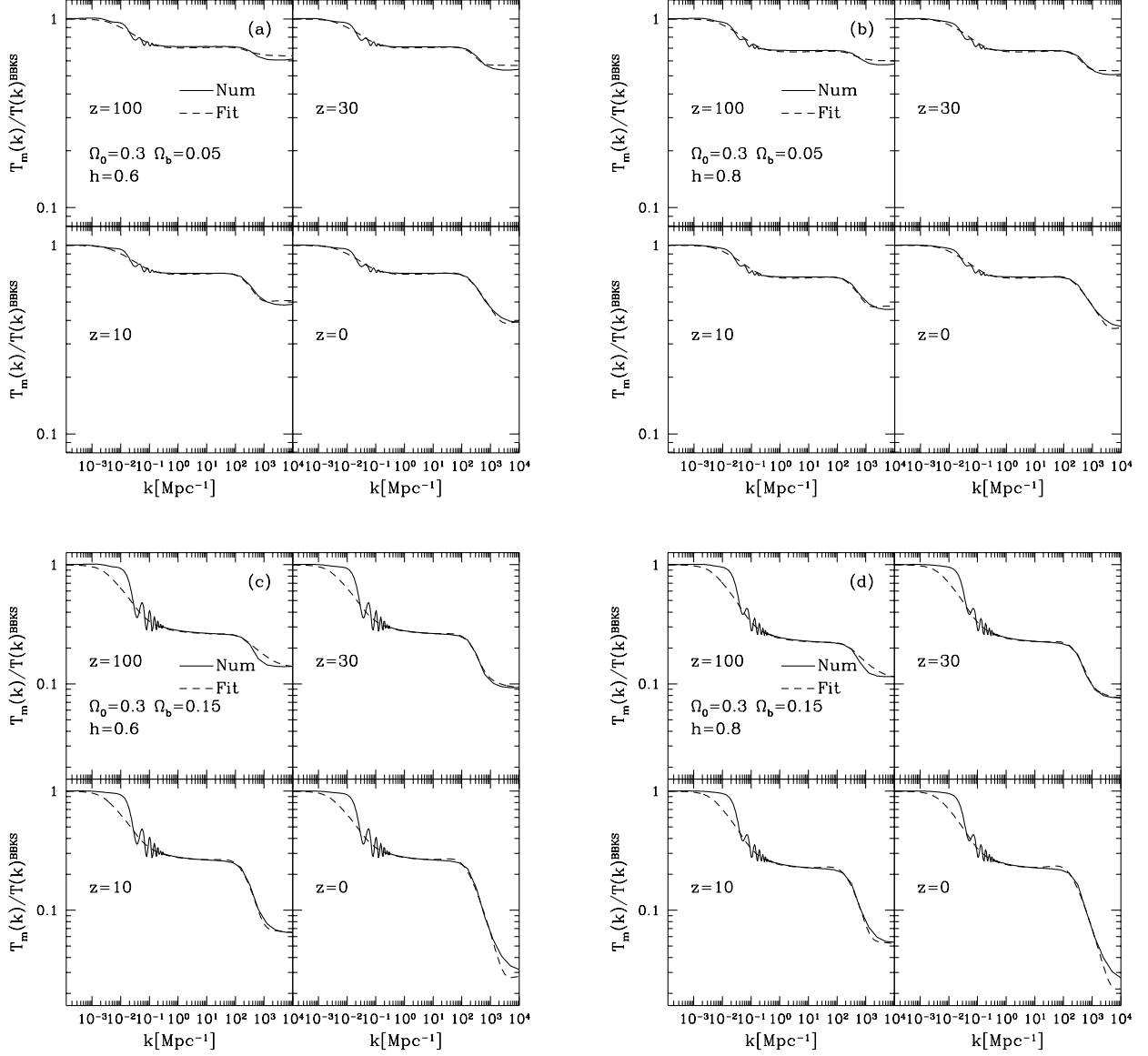


Fig.5.—Transfer functions normalized by the BBKS transfer function $T_m(k)/T^{\text{BBKS}}(k)$. In each panel, the fitting formula is compared with the numerical result. 4 panels in each figure show the time evolution of the transfer function at $z = 100$, $z = 30$, $z = 10$, $z = 0$, respectively.

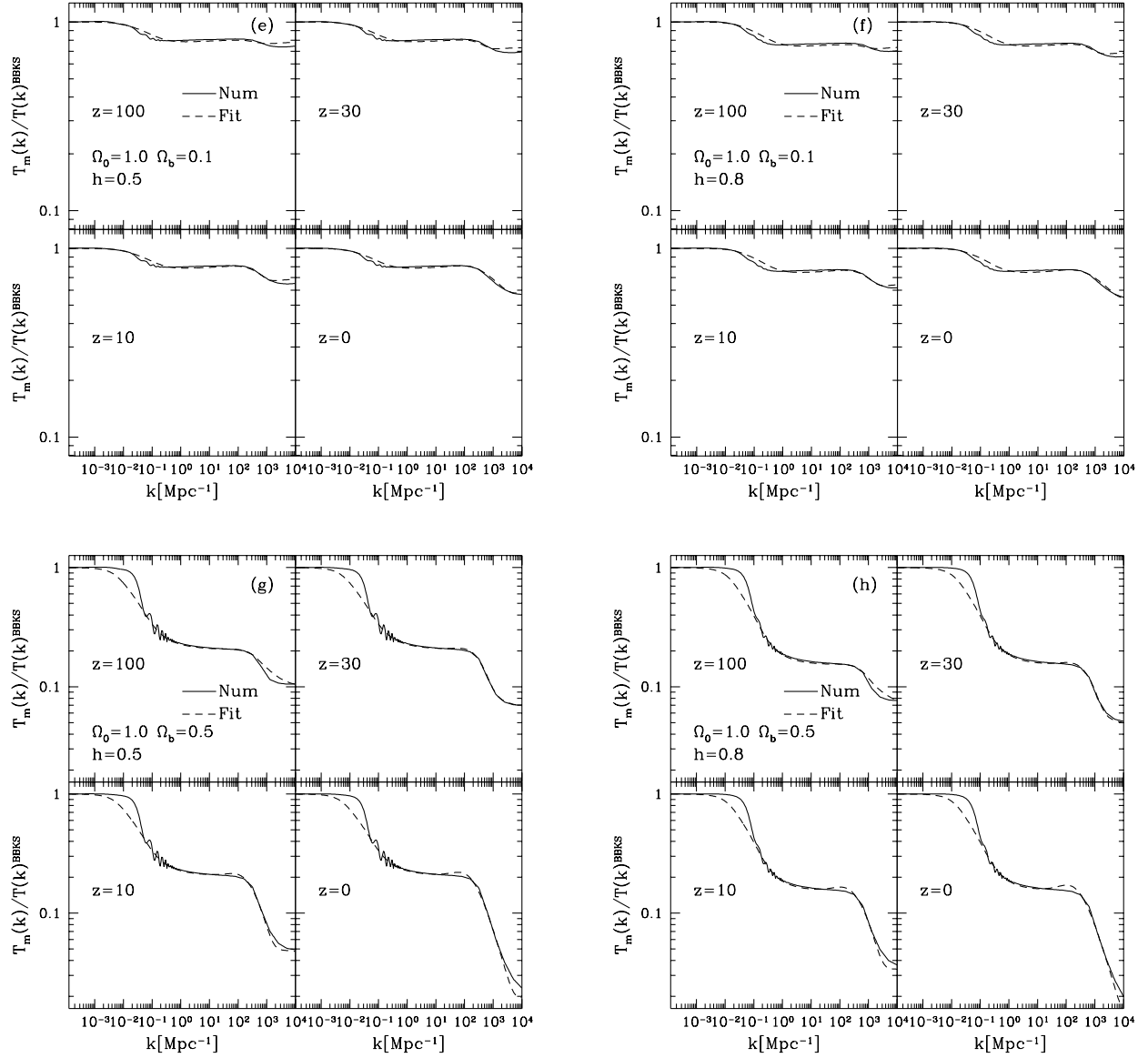


Fig.5.—Continued

6. Simple Demonstrations

In this section, we first show the accuracy of the fitting formula by calculating the following statistical quantities of the large scale structure the universe. Here we consider the CDM cosmology with the Harrison-Zeldovich initial density power spectrum. For low density universe models, we introduce the cosmological constant to keep the flat geometry. Let us introduce σ_R which is defined as

$$\sigma_R^2(a) = \frac{1}{2\pi^2} \int_0^\infty dk k^2 P(a, k) W(kR)^2, \quad (40)$$

where $P(a, k) = \langle \delta_m(a, k)^2 \rangle$ is the power spectrum of the linear density perturbations at time a , and $W(x) = 3(\sin x - x \cos x)/x^3$ is the top-hat window function. To determine the amplitude of the power spectrum, we use the COBE normalization by Bunn & White (1996). According to their results, we can rewrite equation (40) as

$$\sigma_R^2(a) = \left(\frac{D_1(a)}{D_1(a_0)} \right)^2 \delta_H^2 \int_0^\infty \frac{dk}{k} \left(\frac{k}{H_0} \right)^4 T_m(a, k)^2 W(kR)^2, \quad (41)$$

with $\delta_H = 1.94 \times 10^{-5} \Omega_0^{-0.785-0.05 \ln \Omega_0}$ for Λ -models. We note that $D_1(a)$ in equation (41) represents the growing mode solution for matter perturbations taking Λ -term into account, which differs from (A8) at $z \lesssim$ a few due to the Λ -term. For Λ -model, $D_1(a)$ is written as (see e.g., Peebles 1980)

$$D_1(a(1+z)) = \frac{5\Omega_0}{2} \sqrt{\Omega_0(1+z)^3 + 1 - \Omega_0} \int_0^{1/(1+z)} da' \left(\frac{a'}{\Omega_0 + a'^3(1-\Omega_0)} \right)^{3/2}, \quad (42)$$

which is normalized as $D_1(a) \simeq 1/(1+z)$ at $z \gg 1$.

The observational quantity σ_8 is defined as $\sigma_8 = \sigma_{R=8h^{-1}\text{Mpc}}(z=0)$. In Table 1, we show the value of σ_8 by numerical calculations comparing with various transfer functions. In this table, σ_8^N , σ_8^S , σ_8^F , σ_8^{BBKS} and σ_8^{EH} denote values obtained by the numerical calculation, our fitting formula, the empirical scaling by Sugiyama (1995), the original fitting formula by BBKS and the scaling⁵ by Eisenstein & Hu (1997), respectively.

It is shown that our fitting formula together with that obtained by the empirical scalings by the shape parameter Γ by (Sugiyama 1995) and by Eisenstein & Hu (1997), well reproduce the numerical result. This is because that the fitting formulas are designed to cross the center of oscillations.

In order to check the accuracy on small scales, we have calculated the quantities, $\sigma_{R=1h^{-1}\text{Mpc}}(z=3)$, $\sigma_{R=0.1h^{-1}\text{Mpc}}(z=5)$, $\sigma_{R=10^{-2}h^{-1}\text{Mpc}}(z=10)$, and $\sigma_{R=10^{-3}h^{-1}\text{Mpc}}(z=10)$, for various cosmological models. The results are shown in Tables 2-5. From these results, we can find that our fitting formula works very well on small scales.

⁵ Here we used $\Gamma_{\text{eff}}(k)$ in their paper in stead of the usual Γ -factor ($= \Omega_0 h$).

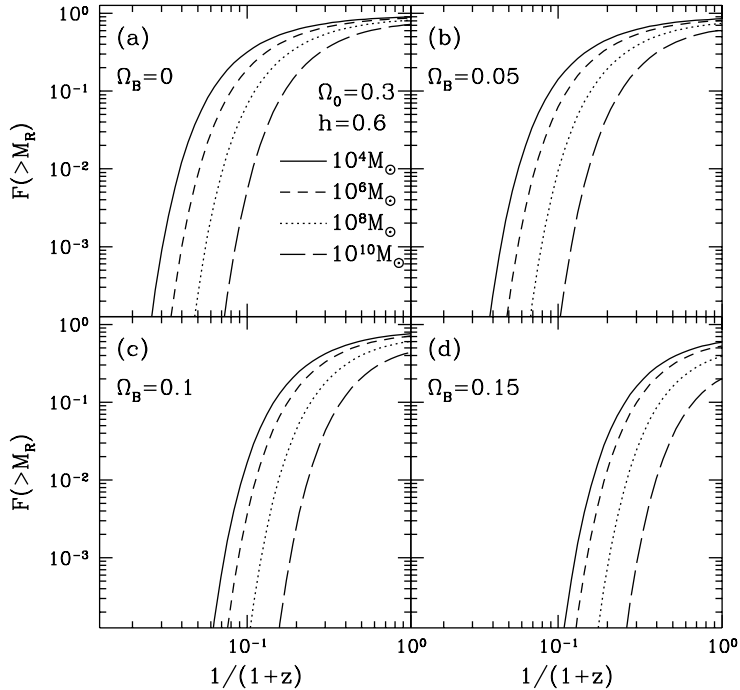


Fig. 6.— Mass fractions of the bound objects $F(> M_R)$. The cosmological parameters taken in this figure is $\Omega_0 = 0.3$ and $h = 0.6$. In each panel the baryon fraction is different, which are: (a) $\Omega_b = 0$; (b) $\Omega_b = 0.05$; (c) $\Omega_b = 0.1$; and (d) $\Omega_b = 0.15$.

Next we briefly demonstrate a cosmological implication of our results. The study of the early formation of collapsed objects and the thermal history of the high- z universe is one of the most important issue in cosmology and galaxy formation. (e.g., Fukugita & Kawasaki 1994; Gnedin & Ostriker 1997; Ostriker & Gnedin 1996; Haiman & Loeb 1997). The statistical arguments allow us to investigate such early history of the formation of small scale cosmic objects in the high- z universe without big numerical calculations. The Press-Schechter theory (Press & Schechter 1974) is among the most simple theory to discuss the statistics of the gravitationally collapsing objects. According to the Press-Schechter formula, we calculate the fractions of the gravitationally bound system, and show the effects of the baryon fraction on the formation rate of the nonlinear objects in the high- z universe.

The Press-Schechter theory predicts that the mass fraction which is gravitationally bounded objects above a given mass M_R at cosmic time a becomes (e.g., Padmanabhan 1993),

$$F(> M_R) = \text{erfc}\left(\frac{\bar{\delta}_c}{\sqrt{2}\sigma(M_R, a)}\right), \quad (43)$$

where $\sigma(M_R, a) \equiv \sigma_R(a)$ is define by equation (41), $M_R = 4\pi\bar{\rho}_0 R^3/3$, $\bar{\rho}_0$ is the spatially averaged matter energy density, and $\bar{\delta}_c = 1.69$. Figure 6 shows the mass fraction $F(> M_R)$ calculated from

equation (43), for the cosmological model $\Omega_0 = 0.3$, $h = 0.6$ with different baryon density fractions. (a) is the case that the baryon fraction is neglected. (b) is the case with including the baryon fraction $\Omega_b = 0.05$. (c) is the case $\Omega_b = 0.1$, and (d) is $\Omega_b = 0.15$. It is apparent that the formation rate of cosmic objects is delayed in a universe with large baryon fraction.

7. Summary and Discussions

In this paper, we have carefully re-investigated the evolution of the small scale density fluctuations in an expanding universe, motivated from the studies of cosmic structure formation in the high- z universe. Under the assumption of the hierarchical clustering scenario, the structure formation takes place from smaller scales. Therefore such careful investigation of the evolution of density fluctuations on small scales is necessary. In the universe with non-negligible baryon fraction, the evolution of density fluctuations is very complicated because baryon perturbations affect CDM perturbations through the gravitational interaction.

Interestingly, baryon density fluctuations show the varieties of physical processes caused by the interaction with photons which are summarized in Figure 2. Discussing the physical scales characterizing these processes, we have studied the evolution of the small scale baryon density perturbations. In this investigation, we have found the growth of baryon density fluctuations on small scales after the diffusion damping and before the decoupling epoch, which is related with the breaking down of the tight coupling approximation between baryons and photons. We have referred this growing mode as the terminal velocity mode.

We have re-analyzed the total matter transfer function. In the universe with non-negligible baryon fraction, the transfer function is changed from the familiar transfer function by BBKS, for $k \gtrsim 0.1\Omega_0^{1/2}\Omega_0^{1/2}h^2$. Extending the previous fitting formulas by Sugiyama (1995) and HS96 with including the Jeans effect after the decoupling epoch which causes the damping on very small scales, we have presented the analytic transfer function in a way of modifying the BBKS transfer function. This fitting function is rather complicated, but its accuracy is very high particularly around the galaxy scale $1\text{Mpc}^{-1} \lesssim k \lesssim 100\text{Mpc}^{-1}$. This fitting function is applicable for the entire range. Even for $k \gtrsim 100\text{Mpc}^{-1}$ it works within $\sim 10\%$ error. Unless one would like to trace the oscillation feature on intermediate scales $0.01\text{Mpc}^{-1} \lesssim k \lesssim 0.1\text{Mpc}^{-1}$ which is caused by the acoustic oscillation by photon-baryon fluid before the decoupling epoch (in this case, one need to employ pure numerical calculations or the newly suggested fitting formula by Eisenstein & Hu (1997)), our fitting works fairly well for the entire range of $k \lesssim 10^4\text{Mpc}^{-1}$.

When discussing the formation epoch of small cosmic objects, the amplitude of density fluctuations is the important factor. In the universe with large baryon density fraction, the amplitude of total matter perturbations is decreased on small scales. Then the formation of the cosmic objects is delayed. Moreover, the evolution of total density fluctuations on these scales does not quite follow the usual growth rate D_1 . We have described this time dependence of the transfer function as f_m .

In a low density universe, the baryon density fraction becomes large relative to the CDM density fraction. Then this effect becomes significant, as demonstrated in §6.

Finally, if once the early re-ionization occurs, baryon density perturbations evolve in a different way. This effect is beyond the scope of this paper. But a recent paper by Chiba, Kawasaki & Sugiyama (1997) showed that the baryon and total matter evolution are affected by the early re-ionization in case of high baryon fraction models.

ACKNOWLEDGMENT

One of us (K.Y.) thanks Y.Kojima and N.Ohno for comments and discussions at the early stage of this work. He also thanks J.Yokoyama and the people at Yukawa Institute and Department of Physics, Kyoto University, Kitashirakawa, Kyoto, where some parts of this work were done, for their hospitality. This work is supported by the Grants-in-Aid for Scientific Research of Ministry of Education, Science and Culture of Japan (Nos. 09740203 and 09440106).

REFERENCES

- Bardeen, J.M., Bond, J.R, Kaiser, N., & Szalay, A.S. 1986 ApJ, 304, 15 (BBKS).
- Bardeen, J. M., Steinhardt, P. J., & Turner, M. S. 1983, Phys. Rev. D28, 679.
- Bunn, E. F. & White, M. 1996, 1997, ApJ, 480, 6.
- Chiba, T., Kawasaki, M., & Sugiyama, N. 1997, preprint.
- Dodelson, S., Gates, E., & Turner, M. S. 1996, Science 274, 69.
- Eisenstein, D. J., & Hu, W. 1997, preprint astro-ph/9709112.
- Fukugita, M. & Kawasaki, M. 1994, MNRAS, 269, 563.
- Gnedin, N. Y., & Ostriker, J. P. 1997, ApJ, 486, 581.
- Haiman, Z., & Loeb, A. 1997, ApJ, 483, 21.
- Holtzman, J. A. ApJS, 71, 1.
- Hu, W., & Sugiyama, N. 1995, ApJ, 444, 489 (HS95).
- Hu, W., & Sugiyama, N. 1996, ApJ, 471, 542 (HS96).
- Jungman, G., Kamionkowski, M., Kosowsky, A., & Spergel, D. N. 1996, Phys. Rev. Lett.76, 1007.
- Kodama, H & Sasaki, M. 1986, Int. J. Mod.Phys. A1, 265.

- Loveday, J. 1996, preprint astro-ph/9605028.
- Ostriker, J. P. & Gnedin, N. Y., 1996, ApJ, 472, L63.
- Padmanabhan, T. 1993, Structure Formation in the Universe, Cambridge University Press.
- Peacock, J. A., & Dodds, S. J. 1994, MNRAS, 267, 1020
- Peebles, P.J.E., 1980, Large-Scale Structure of the Universe, Princeton University Press.
- Peebles, P.J.E., 1993, Principles of Physical Cosmology, Princeton University Press.
- Press, W. H., & Schechter, P. 1974, ApJ, 187, 425.
- Sato, H. 1971, Prog. Theor. Phys. 45, 370.
- Silk, J. 1968, ApJ, 151, 459.
- Strauss, M. A. 1996, astro-ph/9610033, to be published in “Structure Formation in the Universe”, eds. A.Dekel & J.P.Ostriker.
- Sugiyama, N. 1995, ApJS, 100, 281.
- Weinberg, S. 1971, ApJ, 168, 175.
- White, M., Scott, D., & Silk, J. 1994, Annu.Rev.Astro.Astrophys. 32, 319.
- White, M., Scott, D., Silk, J., & Davis, M. 1995, MNRAS276, L69.
- Yamamoto, K., Sugiyama, N., & Sato, H. 1997, Phys. Rev. D in press (YSS).
- Zaldarriaga, M., Spergel, D. N., & Seljak, U. 1997, astro-ph/9702157.

A. Evolution of Matter Perturbations

In this Appendix, we briefly review the analytic formulation of the evolution of the matter perturbations on small scales obtained by HS96. Let us consider the evolution after the diffusion damping. If we set photon and baryon fluctuations to be negligible small (this assumption is valid by the argument in §3.3 even though there exists small fraction of baryon fluctuations after the damping epoch due to the terminal velocity), only CDM contributes to the gravitational potential. Which permits the equation of CDM perturbations to be written as

$$\frac{d^2 \delta_c}{dy^2} + \frac{2 + 3y}{2y(1+y)} \frac{d\delta_c}{dy} = \frac{3}{2y(1+y)} \frac{\Omega_c}{\Omega_0} \delta_c, \quad (\text{A1})$$

where $y \equiv a/a_{\text{eq}}$ and $\Omega_c = \Omega_0 - \Omega_b$. The solutions are given in terms of the Hypergeometric function

$$U_i = (1+y)^{-\alpha_i} {}_2F_1\left(\alpha_i, \alpha_i + 1/2, 2\alpha_i + 1/2; 1/(1+y)\right), \quad (\text{A2})$$

where $i = 1, 2$ and $\alpha_i = (1 \pm \sqrt{1 + 24\Omega_c/\Omega_0})/4$ with $-$ and $+$ for $i = 1$ and 2 , respectively.

With considering the matching conditions to the solution outside the horizon in the radiation dominated stage, the solution for δ_c after the horizon crossing is obtained,

$$\delta_c(\eta, k) = I_1 \Phi(0, k) \left(A_1 U_1(\eta) + A_2 U_2(\eta) \right), \quad (\text{A3})$$

where

$$A_1 = \frac{\Gamma(\alpha_1)\Gamma(\alpha_1 + 1/2)}{\Gamma(2\alpha_1 + 1/2)(\psi(2\alpha_2) - \psi(2\alpha_1))} \left(\frac{1}{2} \ln \left[I_2 \frac{a_{\text{eq}}}{a_{\text{H}}} \right] + \psi(1) - \psi(\alpha_2) + \ln 2 \right), \quad (\text{A4})$$

A_2 is obtained by replacing the subscripts $1 \leftrightarrow 2$, I_1 and I_2 are obtained from the numerical fitting formulas

$$I_1 = 9.11(1 + 0.128f_\nu + 0.029f_\nu^2), \quad (\text{A5})$$

$$I_2 = 0.594(1 - 0.631f_\nu + 0.284f_\nu^2), \quad (\text{A6})$$

$$\frac{a_{\text{H}}}{a_{\text{eq}}} = \frac{1 + \sqrt{1 + 8(k/k_{\text{eq}})^2}}{4(k/k_{\text{eq}})^2}, \quad (\text{A7})$$

and $\psi(x)$ is the poli-gamma function.

After the epoch that the baryon pressure becomes negligible, i.e., the drag epoch z_d or the second Jeans crossing epoch z_j^{out} depends on scales, baryon fluctuations evolve through CDM gravitational potential well. In this stage, it is well known that the matter fluctuations δ_m , defined by equation (34), follow the growing and decaying solutions (Peebles 1980)

$$D_1 = \frac{2}{3} + y, \quad (\text{A8})$$

$$D_2 = \frac{15}{8}(2 + 3y) \ln \left[\frac{(1+y)^{1/2} + 1}{(1+y)^{1/2} - 1} \right] - \frac{45}{4}(1+y)^{1/2}. \quad (\text{A9})$$

These solutions correspond to U_1 and U_2 with $\alpha_i|_{\Omega_c=\Omega_0} = (1 \pm 5)/4$. Matching solutions at $y \equiv y_c = y_d$ or $= y_J^{\text{out}}$, we obtain for the growing mode solution as

$$\delta_m(\eta, k) = \left(G_1 \delta_m - G_2 \dot{\delta}_m \right) \Big|_{y=y_c} D_1(y(\eta)), \quad (\text{A10})$$

with

$$G_1 = \frac{\dot{D}_2}{D_1 \dot{D}_2 - \dot{D}_1 D_2}, \quad G_2 = \frac{D_2}{D_1 \dot{D}_2 - \dot{D}_1 D_2}. \quad (\text{A11})$$

B. Effect of the baryon thermal pressure on the Transfer Function

In this Appendix we describe some details which are important to construct an analytic transfer function on very small scales, $k > 1 \text{Mpc}^{-1}$. We first note the small scale transfer function obtained in HS96. According to their result, the fitting formula of the CDM transfer function is written as,

$$T_c(a, k) = \alpha \frac{\ln[1.8\beta q]}{14.2q^2}, \quad (\text{B1})$$

with

$$\alpha = a_1^{-\Omega_b/\Omega_0} a_2^{-(\Omega_b/\Omega_0)^3}, \quad \beta^{-1} = 1 + b_1((\Omega_c/\Omega_0)^{b_2} - 1), \quad (\text{B2})$$

$$\begin{aligned} a_1 &= (46.9\Omega_0 h^2)^{0.670} (1 + (32.1\Omega_0 h^2)^{-0.532}), \\ a_2 &= (12.0\Omega_0 h^2)^{0.424} (1 + (45.0\Omega_0 h^2)^{-0.582}), \\ b_1 &= 0.944 (1 + (458.0\Omega_0 h^2)^{-0.708})^{-1}, \\ b_2 &= (0.395\Omega_0 h^2)^{-0.0266}, \end{aligned}$$

and $q = k(\text{Mpc}^{-1}\Omega_0 h^2)^{-1}(T_0/2.7\text{K})^2$. Though this formula is rather complicated, it works to 1% accuracy. We should notice that this formula is applicable only on small scales, $k \gtrsim 1 \text{Mpc}^{-1}$.

Let us describe the function $f_m(a, k)$ in equation (37). As we have shown in Appendix A, δ_m grows in proportion to $D_1(a)$ after the pressure becomes ineffective. On scales larger than the Jeans scale at the decoupling epoch, i.e., $k < k_{\text{JP}}$, the photon pressure becomes ineffective after the decoupling epoch. Then δ_m evolves in proportion to $D_1(a)$. Once the matter fluctuations become to follow this growing mode solution, the transfer function becomes independent of time. Therefore on these scales, the transfer function does not change its shape after the drag epoch. On scales $k \gtrsim k_{\text{JP}}$, on the other hand, the baryon thermal pressure keeps the perturbations from growing even after the decoupling of baryons from photons. As we have seen in Appendix A, the growth rate of CDM fluctuations is suppressed in the situation that there exists a homogeneous matter (baryon) component besides the CDM component. This effect alters the transfer function on small scales $k \gtrsim k_{\text{JP}}$ even after the decoupling epoch. The function $f_m(a, k)$ is multiplied in order to describe this effect.

In order to find the analytic form of $f_m(a, k)$, we rewrite

$$T_m(a, k) = T_m(a_d, k) \frac{T_m(a, k)}{T_m(a_d, k)} \equiv T_m(a_d, k) f(a, k), \quad (\text{B3})$$

where a_d denotes the scale factor at the decoupling epoch. Thus $f(a, k)$ is defined as the ratio of the transfer function at $a(\eta)$ to that at the decoupling time. From the definition of the transfer function (35), we can rewrite

$$f(a, k) = \frac{D_1(a_d) \delta_m(a, k)}{D_1(a) \delta_m(a_d, k)}. \quad (\text{B4})$$

We first consider the case $k < k_{\text{JP}}$. This case is trivial, because δ_m grows in proportion to $D_1(a)$ after the decoupling, as described before. Then we get $f(a, k) = 1$.

We next consider the case $k > k_{\text{JP}}$. These perturbations stay inside the Jeans scale until $a_{\text{J}}^{\text{out}}/a_{\text{eq}} = y_{\text{J}}^{\text{out}}$, which is defined in equation (33). Assuming that baryon density fluctuations do not contribute to the gravitational potential in this regime, we approximate the growth rate of the CDM density perturbations by the growing mode solution $U_1(a)$ in equation (A2). After the decoupling epoch, we can assume the matter domination of the universe, i.e., $a/a_{\text{eq}} \gg 1$. Hence we further approximate $U_1(a) \simeq (1 + a/a_{\text{eq}})^{\alpha_1}$ with $\alpha_1 = (1 - \sqrt{1 + 24\Omega_c/\Omega_0})/4$ as is shown in Appendix A. Then we can write

$$f(a, k) \simeq \frac{D_1(a_d) U_1(a)}{D_1(a) U_1(a_d)} \simeq \left(\frac{1 + y_d}{1 + y} \right)^{1+\alpha_1}, \quad (y < y_{\text{J}}^{\text{out}}), \quad (\text{B5})$$

where $y = a/a_{\text{eq}}$ and $y_d = a_d/a$ as are defined before. After the Jeans crossing $a/a_{\text{eq}} > y_{\text{J}}^{\text{out}}$, we approximate that δ_m follows the growing mode $D_1(a)$ and that the solution is given by equation (A10) with replacing y_c by $y_{\text{J}}^{\text{out}}$. Then we can write

$$\begin{aligned} f(a, k) &\simeq \frac{D_1(a_d)}{U_1(a_d)} \left(G_1(a) U_1(a) - G_2(a) \dot{U}_1(a) \right) \Big|_{a/a_{\text{eq}} = y_{\text{J}}^{\text{out}}} \\ &\simeq \frac{3 - 2\alpha_1}{5} \left(\frac{1 + a_d/a_{\text{eq}}}{1 + y_{\text{J}}^{\text{out}}} \right)^{1+\alpha_1}, \quad (a/a_{\text{eq}} > y_{\text{J}}^{\text{out}}). \end{aligned} \quad (\text{B6})$$

Here we have assumed that the amplitude of δ_b is small at $y_{\text{J}}^{\text{out}}$.

Summarizing the results, $f(a, k)$ is evaluated

$$f(a, k) \simeq \begin{cases} 1 & (k < k_{\text{JP}}), \\ \left((1 + y_d)/(1 + y) \right)^{\alpha_1+1} & (k > k_{\text{JP}} \text{ and } y < y_{\text{J}}^{\text{out}}), \\ \left((1 + y_d)/(1 + y_{\text{J}}^{\text{out}}) \right)^{\alpha_1+1} (3 - 2\alpha_1)/5 & (k > k_{\text{JP}} \text{ and } y > y_{\text{J}}^{\text{out}}). \end{cases}$$

In the case when the baryon fraction is negligible, i.e., $\Omega_b \ll \Omega_0$, we have $\alpha_1 = -1$ and $f(a, k) = 1$. On the other hand, in the cosmological models with the non-negligible baryon fraction, the growth rate of CDM fluctuations is suppressed even after the decoupling. And the matter transfer function is changed.

Combining above $f(a, k)$'s on difference scales, we give the next fitting function,

$$f_{\text{m}}(a, k) = \frac{1}{(k/\tilde{k}_{\text{JP}})^{1.3} + 1} + \frac{1}{(\tilde{k}_{\text{JP}}/k)^{1.3} + 0.9} \left[\frac{1}{(y/y_{\text{J}}^{\text{out}})^{1.3} + 1} \left(\frac{1 + y_{\text{d}}}{1 + y} \right)^{\alpha_1 + 1} + \frac{1}{(y_{\text{J}}^{\text{out}}/y)^{1.3} + 1} \frac{3 - 2\alpha_1}{5} \left(\frac{1 + y_{\text{d}}}{1 + y_{\text{J}}^{\text{out}}} \right)^{\alpha_1 + 1} \right], \quad (\text{B7})$$

with

$$\tilde{k}_{\text{JP}} = 350(1 + 50 (y_{\text{d}}/y))(\Omega_0 h^2)^{1/2} \text{Mpc}^{-1}, \quad (\text{B8})$$

$$y_{\text{d}} = 20\Omega_0 h^2 (\Omega_{\text{b}} h^2)^{-0.034}, \quad (\text{B9})$$

and $y = a/a_{\text{eq}} = 2.4 \times 10^4 (1+z)^{-1} \Omega_0 h^2$. Here we determine numerical constant factors to reproduce the numerical computations. The reason why we employ \tilde{k}_{JP} instead of k_{JP} is following. Even on scales smaller than k_{JP} , the thermal pressure cannot entirely prevent baryon fluctuations from the growth because of the existence of the CDM potential. A certain amount of the growth rate has to be taken into account at $k \gtrsim k_{\text{JP}}$ even though the rate is less than D_1 .

Table 1. $\sigma_{R=8h^{-1}\text{Mpc}}$ for various cosmological models.

Ω_0	Ω_b	h	$\sigma_{8h^{-1}\text{Mpc}}^{\text{N}}$	$\sigma_{8h^{-1}\text{Mpc}}^{\text{F}}$	$\sigma_{8h^{-1}\text{Mpc}}^{\text{S}}$	$\sigma_{8h^{-1}\text{Mpc}}^{\text{BBKS}}$	$\sigma_{8h^{-1}\text{Mpc}}^{\text{EH}}$
0.3	0.05	0.6	0.70	0.71	0.70	0.95	0.71
0.3	0.1	0.6	0.51	0.51	0.51	0.95	0.50
0.3	0.15	0.6	0.35	0.33	0.37	0.95	0.34
0.3	0.2	0.6	0.23	0.19	0.26	0.95	0.22
0.3	0.05	0.8	0.98	1.00	0.98	1.36	0.99
0.3	0.1	0.8	0.68	0.69	0.70	1.36	0.68
0.3	0.15	0.8	0.46	0.44	0.49	1.36	0.44
0.3	0.2	0.8	0.29	0.24	0.34	1.36	0.28
1.0	0.05	0.5	1.18	1.22	1.18	1.31	1.21
1.0	0.1	0.5	1.08	1.12	1.06	1.31	1.11
1.0	0.5	0.5	0.50	0.46	0.41	1.31	0.48
1.0	0.05	0.8	1.83	1.92	1.87	2.07	1.90
1.0	0.1	0.8	1.65	1.76	1.68	2.07	1.73
1.0	0.5	0.8	0.74	0.66	0.62	2.07	0.70

^a $\sigma^{\text{N}}, \sigma^{\text{F}}, \sigma^{\text{S}}, \sigma^{\text{BBKS}}$, and σ^{EH} are calculated by the full numerical computation, using our analytic fitting, an analytic fitting by Sugiyama (1995), the one by BBKS and the one by Eisenstein & Hu (1997) with employing their empirical scalings of the shape parameter Γ , respectively.

Table 2. $\sigma_{R=1h^{-1}\text{Mpc}}$ at $z = 3$

Ω_0	Ω_b	h	$\sigma_{1h^{-1}\text{Mpc}}^{\text{N}}$	$\sigma_{1h^{-1}\text{Mpc}}^{\text{F}}$	$\sigma_{1h^{-1}\text{Mpc}}^{\text{S}}$	$\sigma_{1h^{-1}\text{Mpc}}^{\text{BBKS}}$	$\sigma_{1h^{-1}\text{Mpc}}^{\text{EH}}$
0.3	0.05	0.6	0.66	0.66	0.64	0.92	0.65
0.3	0.1	0.6	0.44	0.44	0.44	0.92	0.43
0.3	0.15	0.6	0.28	0.27	0.30	0.92	0.26
0.3	0.2	0.6	0.16	0.15	0.20	0.92	0.14
0.3	0.05	0.8	1.00	0.99	0.96	1.45	0.97
0.3	0.1	0.8	0.64	0.63	0.64	1.45	0.61
0.3	0.15	0.8	0.38	0.37	0.42	1.45	0.36
0.3	0.2	0.8	0.20	0.19	0.27	1.45	0.19
1.0	0.05	0.5	1.31	1.31	1.25	1.45	1.29
1.0	0.1	0.5	1.16	1.16	1.08	1.45	1.15
1.0	0.5	0.5	0.37	0.37	0.31	1.45	0.36
1.0	0.05	0.8	2.51	2.53	2.44	2.86	2.51
1.0	0.1	0.8	2.18	2.21	2.07	2.86	2.18
1.0	0.5	0.8	0.58	0.57	0.53	2.86	0.56

^a $\sigma^{\text{N}}, \sigma^{\text{F}}, \sigma^{\text{S}}, \sigma^{\text{BBKS}}$, and σ^{EH} are same as Table 1.

Table 3. $\sigma_{R=0.1h^{-1}\text{Mpc}}$ at $z = 5$

Ω_0	Ω_b	h	$\sigma_{0.1h^{-1}\text{Mpc}}^{\text{N}}$	$\sigma_{0.1h^{-1}\text{Mpc}}^{\text{F}}$	$\sigma_{0.1h^{-1}\text{Mpc}}^{\text{S}}$	$\sigma_{0.1h^{-1}\text{Mpc}}^{\text{BBKS}}$	$\sigma_{0.1h^{-1}\text{Mpc}}^{\text{EH}}$
0.3	0.05	0.6	0.94	0.93	0.88	1.32	0.89
0.3	0.1	0.6	0.61	0.60	0.59	1.32	0.57
0.3	0.15	0.6	0.36	0.36	0.39	1.32	0.33
0.3	0.2	0.6	0.19	0.19	0.26	1.32	0.17
0.3	0.05	0.8	1.47	1.46	1.38	2.16	1.39
0.3	0.1	0.8	0.91	0.90	0.88	2.16	0.84
0.3	0.15	0.8	0.51	0.51	0.56	2.16	0.47
0.3	0.2	0.8	0.25	0.25	0.35	2.16	0.24
1.0	0.05	0.5	2.26	2.23	2.08	2.47	2.16
1.0	0.1	0.5	1.98	1.95	1.76	2.47	1.89
1.0	0.5	0.5	0.55	0.55	0.45	2.47	0.51
1.0	0.05	0.8	4.83	4.75	4.48	5.41	4.63
1.0	0.1	0.8	4.13	4.06	3.71	5.41	3.93
1.0	0.5	0.8	0.93	0.91	0.80	5.41	0.84

^a $\sigma^{\text{N}}, \sigma^{\text{F}}, \sigma^{\text{S}}, \sigma^{\text{BBKS}}$, and σ^{EH} are same as Table 1.

Table 4. $\sigma_{R=10^{-2}h^{-1}\text{Mpc}}$ at $z = 10$

Ω_0	Ω_b	h	$\sigma_{10^{-2}h^{-1}\text{Mpc}}^{\text{N}}$	$\sigma_{10^{-2}h^{-1}\text{Mpc}}^{\text{F}}$	$\sigma_{10^{-2}h^{-1}\text{Mpc}}^{\text{S}}$	$\sigma_{10^{-2}h^{-1}\text{Mpc}}^{\text{BBKS}}$	$\sigma_{10^{-2}h^{-1}\text{Mpc}}^{\text{EH}}$
0.3	0.05	0.6	0.85	0.85	0.79	1.20	0.80
0.3	0.1	0.6	0.54	0.54	0.52	1.20	0.50
0.3	0.15	0.6	0.32	0.32	0.34	1.20	0.29
0.3	0.2	0.6	0.16	0.16	0.22	1.20	0.14
0.3	0.05	0.8	1.37	1.36	1.26	2.02	1.27
0.3	0.1	0.8	0.82	0.83	0.79	2.02	0.75
0.3	0.15	0.8	0.45	0.46	0.49	2.02	0.41
0.3	0.2	0.8	0.22	0.22	0.31	2.02	0.20
1.0	0.05	0.5	2.28	2.25	2.05	2.46	2.14
1.0	0.1	0.5	1.98	1.96	1.72	2.46	1.85
1.0	0.5	0.5	0.52	0.53	0.41	2.46	0.47
1.0	0.05	0.8	5.12	5.04	4.63	5.65	4.79
1.0	0.1	0.8	4.34	4.28	3.79	5.65	4.03
1.0	0.5	0.8	0.91	0.93	0.75	5.65	0.79

^a $\sigma^{\text{N}}, \sigma^{\text{F}}, \sigma^{\text{S}}, \sigma^{\text{BBKS}}$, and σ^{EH} are same as Table 1.

Table 5. $\sigma_{R=10^{-3}h^{-1}\text{Mpc}}$ at $z = 10$

Ω_0	Ω_b	h	$\sigma_{10^{-3}h^{-1}\text{Mpc}}^{\text{N}}$	$\sigma_{10^{-3}h^{-1}\text{Mpc}}^{\text{F}}$	$\sigma_{10^{-3}h^{-1}\text{Mpc}}^{\text{S}}$	$\sigma_{10^{-3}h^{-1}\text{Mpc}}^{\text{BBKS}}$	$\sigma_{10^{-3}h^{-1}\text{Mpc}}^{\text{EH}}$
0.3	0.05	0.6	1.16	1.15	1.15	1.77	1.17
0.3	0.1	0.6	0.68	0.68	0.75	1.77	0.72
0.3	0.15	0.6	0.38	0.38	0.49	1.77	0.41
0.3	0.2	0.6	0.19	0.19	0.32	1.77	0.20
0.3	0.05	0.8	1.88	1.86	1.86	3.02	1.88
0.3	0.1	0.8	1.05	1.04	1.15	3.02	1.10
0.3	0.15	0.8	0.55	0.55	0.71	3.02	0.59
0.3	0.2	0.8	0.25	0.26	0.44	3.02	0.29
1.0	0.05	0.5	3.48	3.47	3.16	3.80	3.29
1.0	0.1	0.5	2.97	2.94	2.63	3.80	2.83
1.0	0.5	0.5	0.69	0.70	0.60	3.80	0.69
1.0	0.05	0.8	8.05	8.00	7.30	8.97	7.56
1.0	0.1	0.8	6.68	6.62	5.93	8.97	6.32
1.0	0.5	0.8	1.23	1.25	1.12	8.97	1.18

^a $\sigma^{\text{N}}, \sigma^{\text{F}}, \sigma^{\text{S}}, \sigma^{\text{BBKS}}$, and σ^{EH} are same as Table 1.